JHI JOURNAL OF HEALTH INFORMATICS

Automatic detection of pathological retinal images using color and shape features

Detecção automática de imagens de retinas patológicas utilizando características de cor e forma

Detección automática de imágenes patológicas de retina con uso del color y características de forma

Flávio Henrique Duarte de Araújo[1], Rodrigo de Melo Souza Veras[2], Romuere Rodrigues Veloso e Silva[1], André Macedo Santana[2], Fátima Nelsizeuma Sombra de Medeiros[1]

ABSTRACT

Keywords: Machine Learning; Diagnostic Imaging; Exudates and Transudates

Objective: We propose an algorithm for exudate detection and pathological retinal images identification. **Method:** We improved an existing algorithm that detects exudates in a retinal image replacing the k-means clustering by fuzzy k-means and applied an additional step to detect optical disc (OD). Furthermore, our approach added a classification process to eliminate remaining false exudate regions. Finally, we classify the retinal image as pathological or non-pathological by measuring the ratio of candidate exudate regions before classification and the number of regions removed by the classification step. **Results:** Tests were performed on DIARETDB1 database, and the results obtained were; Fmeasure – 90%, area under the ROC curve – 88% and the Kappa coefficient – 77% (very good). **Conclusion:** The success of the algorithm is due mostly to the OD detection approach and the classification step. The obtained results confirmed that the proposed algorithm outperformed the others.

RESUMO

Descritores: Aprendizado de Máquina; Diagnóstico por imagem; Exsudatos e Transudatos

Objetivo: Propor um algoritmo capaz de detectar exsudatos e identificar imagens de retinas patológicas. **Método:** Nós aprimoramos um método de detecção de exsudatos existente na literatura alterando o algoritmo k-means pela sua versão *fuzzy* e realizamos a detecção do disco óptico (DO). Além disso, a proposta adiciona uma fase de classificação para eliminar falsas regiões de exsudatos. Por fim, classificamos as imagens de retina como patológicas ou não-patológicas pelo cálculo da razão entre as regiões candidatas a exsudatos existentes antes e depois da classificação. **Resultados:** Os testes foram realizados nas imagens da base DIARETDB1 e os resultados obtidos foram: *Fmeasure* – 90%, área sobre a curva ROC – 88% e índice Kappa – 77% (muito bom). **Conclusão:** O sucesso do algoritmo deve-se à detecção do DO e à fase de classificação. Os resultados obtidos confirmam que o algoritmo proposto superou os métodos presentes na literatura.

RESUMEN

Descriptores: Aprendizaje automático; Diagnóstico por imagen; Exudados y Transudatos

Objetivo: Proponer un algoritmo para detectar exudados e identificar imágenes de retina patológicas. **Método**: Hemos mejorado un método de detección de exudados existentes en la literatura alterando el algoritmo k-means para su versión difusa y realizamos la detección del disco óptico (DO). Además, la propuesta añade una etapa de clasificación para eliminar los falsos exudados. Finalmente, clasificamos las imágenes de la retina como patológicas o no patológicas mediante el cálculo de el cociente de las regiones candidatas a exudados existentes antes y después de la clasificación. **Resultados**: Los ensayos se realizaron en la base de imágenes DIARETDB1 y los resultados obtenidos fueron: Fmeasure - 90%, área bajo la curva ROC- 88% y el índice Kappa - 77% (muy bueno). **Conclusión**: El éxito del algoritmo se ha debido a la detección del DO y la fase de clasificación. Los resultados confirman que el algoritmo propuesto superó los métodos en la literatura.

[1] *Teleinformatic Engineering Department, Federal University of Ceará - UFC, Fortaleza (CE), Brazil.*
[2] *Computation Department, Federal University of Piauí - UFPI, Teresina (PI), Brazil.*

Autor Correspondente: **Flávio Henrique Duarte de Araújo**
e-mail: **flavio86@ufpi.edu.br**

INTRODUCTION

Digital fundus images can provide information about pathological changes caused by eye and systemic diseases such as hypertension, arteriosclerosis and diabetes mellitus[1]. The retina is the most internal membrane of the eye, and digital image processing techniques can be used to detect changes in retina images. Over the past decade, these techniques have been widely used to identify eye pathologies, including diabetic retinopathy (DR), macular edema and glaucoma[2].

The World Health Organization estimates that 135 million people have diabetes worldwide and that the number of diabetics is expected to increase to 300 million by the year 2025[3]. DR is the largest cause of vision loss in diabetics[4]. An ophthalmologist or other trained health professional diagnoses DR. The accuracy of the diagnosis depends on factors such as image quality and the specialist skill and experience. Thus, an automatic system for the diagnosis of diseases of the visual system using retinal images can reduce the workload of medical professionals.

This disease occurs as a result of vascular changes in the retina, causing swelling of capillaries known as microaneurysms (MA). With the progress of this disease, MAs can rupture and, eventually, become a source of extravasation of plasma, creating regions of fat deposits in the retina known as exudates[2]. Figure 1 shows an example of such lesions.

Greater proximity between the exudates and the macula indicates a more severe stage of the disease because the images captured by the human eye are formed in the macula and any damage in this region can cause vision loss in the patient. The presence of exudates in this region also indicates the presence of another disease called diabetic macular edema[2]. Continuous monitoring of DR is very important because the disease can be diagnosed before the onset of symptoms and early treatment may prevent or reduce vision loss. Several methods for exudate detection are available in the literature, and there are several problem-solving strategies[4].

Garcia et al.[5] applied multilevel thresholding to extract the optical disc (OD) and exudates and classified it using a multilayer perceptron (MLP) and a support vector machine (SVM). They reported that the low quality of the images might interfere in the correct separation of bright from dark lesions. This interference occurs due to the threshold values, region seed points, and stopping criteria are difficult to select automatically.

The algorithms introduced by Sopharak et al.[4] and Harangi et al.[6] provided a pixel-by-pixel classification to determine whether a pixel belongs to an exudate region. The former was applied via an SVM and the latter via an improved Naive-Bayes classifier. Despite the good performance reported, the use of a pixel-by-pixel classification approach requires high computational power for training and classification processes.

Welfer et al.[7] proposed an exudate-detection method based on mathematical morphology techniques. After performing a contrast enhancement in the Luv color space, they carried out several morphological operations, including morphological reconstruction and regional minimum detection, to detect exudates. Akram et al.[8] implemented a set of morphological operations to find the candidate exudate regions. These regions were classified as exudates or non-exudate areas using a hybrid classifier composed of an SVM and Gaussian mixture models. The quality of these methods depends mainly on a structural element and appropriate threshold separating the exudates from the image background. Thus, the morphological reconstruction techniques were sensitive to image contrast variations and non-uniform illumination, thus requiring a pretreatment (e.g., adjusting the lighting).

Rocha et al.[9] proposed a technique based on a visual word dictionary which consists of points of interest (PoIs) located within regions marked by specialists. This technique associates these regions with DR and classifies the fundus images by associating the presence or absence of these PoIs with a DR-related pathology or a normal pattern.

The goal of this paper is to develop algorithms for exudate detection that are capable of classifying a retinal image into a normal or abnormal pattern. Hence, these algorithms may improve the diagnosis quality and decrease the workload of medical professionals. To assess their performance, we tested different classification algorithms that identify exudate regions and pathological images. The
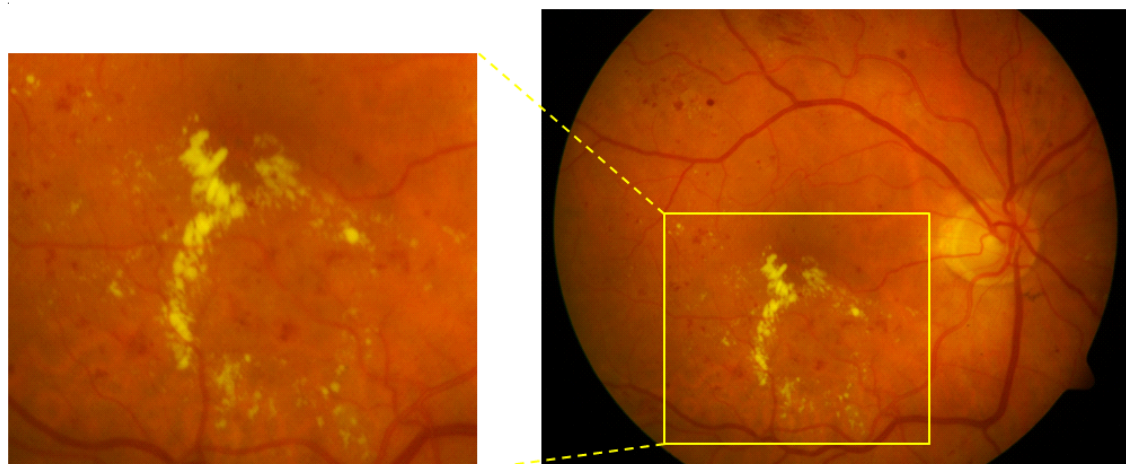

Figure 1 - Example of a retinal image showing exudates.

general methodology consists of three steps: clustering pixels, clustering selection and removal of false candidates. The extended algorithm applies the fuzzy k-means algorithm to gather pixels into clusters and remove false candidates by detecting the OD as the convergence point of the blood vessels. Then, it applies a classification step to the segmented image as a post-processing task. After detecting exudates, the algorithm classifies the retinal image as a pathological or non-pathological pattern.

The remainder of this paper is organized as follows. In Section 2, we describe the materials and methods used in our experiments. Section 3 presents the proposed system. Section 4 shows the results, and in Section 5 we draw conclusions and summarize our contributions.

METHODS

Our paper extends and modifies the exudate detection method proposed by Ram and Sivaswamy[10]. Figure 2 illustrates the general methodology.

The first step of the methodology applies a k-means clustering algorithm to the attributes extracted from the retinal images. At first, it converts the RGB retinal images to three color spaces: Luv, HSV, HSI [18] from which two feature vectors $f_1 = (H, S, V, I)$ and $f_2 = (R, G, L, u, v)$ are extracted. These vectors are the inputs of the k-means algorithm and the clustering output consists of two images (I_1 and I_2).

From images I_1 and I_2, the algorithm selects the clusters that represent the exudate regions. The clusters corresponding to bright lesions and bright backgrounds are in image I_1. Considering that these regions are the brightest, the algorithm selects the cluster in the original image with the highest intensity value I in the HSI space. The clusters in I_2 correspond to the OD and exudates. Thus, the algorithm tracks the yellow regions by selecting the cluster with the smallest á value in the RGB color space, where á = max(R) - max(G). To improve the exudate detection, the algorithm generates two new images: I_3 and I_4. The former consists of all I_1 regions

present in I_2 and the second assembles other I_1 regions not present in I_2.

After performing these steps, it is possible to observe parts of the OD and retinal bright regions marked as exudates. The main characteristic of these regions is that they are bounded and cut across by blood vessels, and they should therefore be identified and removed.

Here, Ram and Sivaswamy[10] remove exudate regions by decorrelating RGB bands and therefore improving vessel contrast. After this task, the vessel region presents the highest values of the component (R). By contrast, the exudate areas and bright regions have the highest values of the component (G). Therefore, if the average values of the pixels of each object in component (R) are higher than the average values of these objects in the original image, they are removed. The objects that belong to the OD region can be eliminated because the larger vessels of the retina are in this region.

At the end of this process, the algorithm proposed by Ram and Sivaswamy[10] applies the Otsu method to the two resulting images to generate the final result. Then, objects present in this image are considered exudates. When the thresholding process removes all image regions, the original image is considered healthy, i.e., without exudates.

PROPOSED SYSTEM

Sometimes the original algorithm classifies isolated pixels and OD regions as exudates. This error may result from the clustering process or false-candidate-removal step. Thus, our paper extends and modifies the original algorithm to correct this problem. It is worth mentioning that the algorithm of Ram and Sivaswamy[10] does not provide classification process. The diagram in Figure 3 displays the proposed methodology.

A. Clustering and Clustering Selection

In contrast to the original version, the proposed methodology for exudate detection applies a fuzzy k-means algorithm instead of the k-means. The reason for
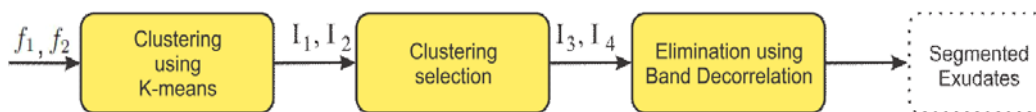

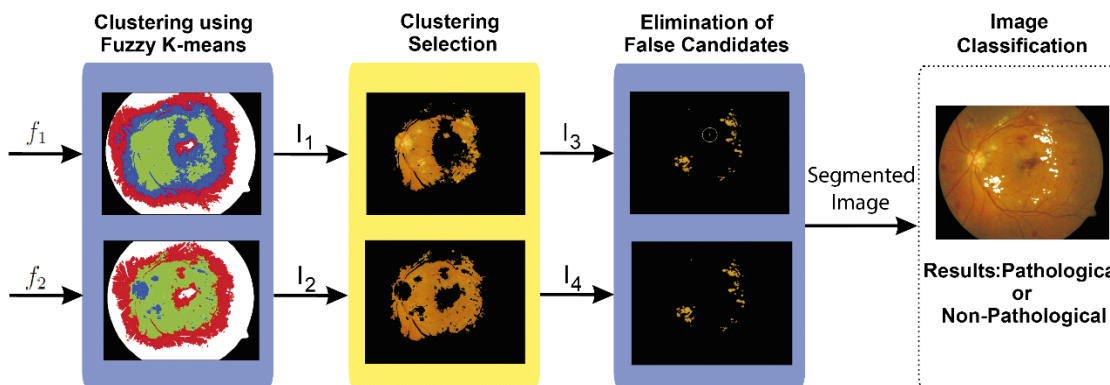**Figure 2 -** Diagram of the algorithm proposed by Ram and Sivaswamy[10].

Figure 3 - Diagram of the proposed system. Blue frames indicate the modified steps of the original algorithm.

choosing it is that the fuzzy k-means algorithm is less susceptible to misclustering caused by illumination differences in retina images.

At first, the parameter adjustment of the fuzzy k-means followed the approach introduced by Sopharak et al[4]. Namely fuzzy degree equal to 2, number of iterations 200 and maximum error of 10^{-6}. Subsequently, variations of these parameters were tested in order to adjusting values for which the results of grouping did not change with them. Thus, the fuzzy degree remained unchanged, the maximum number of iterations was set to 2000 and the maximum error was 10^{-8}. These empirical choice guarantees that the randomness of choosing the initial clusters does not interfere in the final clustering result. In our exhaustive tests, the algorithm always converged to the same result independent of the initial clusters.

B. Elimination of false candidates

Optic Disc Detection: The main challenge in detecting exudates is to distinguish them from the OD because they are similar in shape and color. We used this technique because strategies that select the OD as the region of convergence of the vessels are more successful than those ones based only on color properties. Regarding the vessel-detection step, we applied the algorithm proposed by Zana and Klein[11] to the original image (I_O), and it outputs a vessel image (I_V).

Thereafter, the proposed algorithm converts the image Iv into straight lines by applying Skeletonization and Hough transform (resulting in I_l). Next, it searches for square windows with each side equal to half the radius of the OD (70 pixels), with the most straights in I_l. The OD center is chosen as the center of the window that has more white pixels in Iv. This choice is based on the fact that the vessels that converge to the OD are of greater caliber. The OD-elimination step consists of removing the region connected to the center of the window. Figure 4 shows step by step OD detection.

Candidate Classification: In this study, the Classification step attempted to eliminate remaining false-candidate regions. The classifiers were C4.5, K-Nearest Neighbor (KNN), Multilayer Perceptron (MLP), Radial Basis Function (RBF), RandomForest (RF), RandomTree (RT) and Support Vector Machine (SVM). Details of these classifiers can be found in the papers introduced by Rokach and Oded[12] and Haykin[13].

We tested the classifiers using classical image features, which are divided into two groups: non-color (6 features: area, perimeter, circularity, homogeneity and x and y coordinates of the region center) and color (18 features: average and standard deviation of all components of the color models RGB, Luv and HSI). However, tests have shown that the performance of the classifiers improved when the final set of features was reduced to 12 (5 from the non-color group and 7 from the color group). This set of features consists of area, perimeter, circularity, average of components (L), (u), (v), (H), (I), (G), standard deviation of the component (G), and x and y coordinates of the region center.
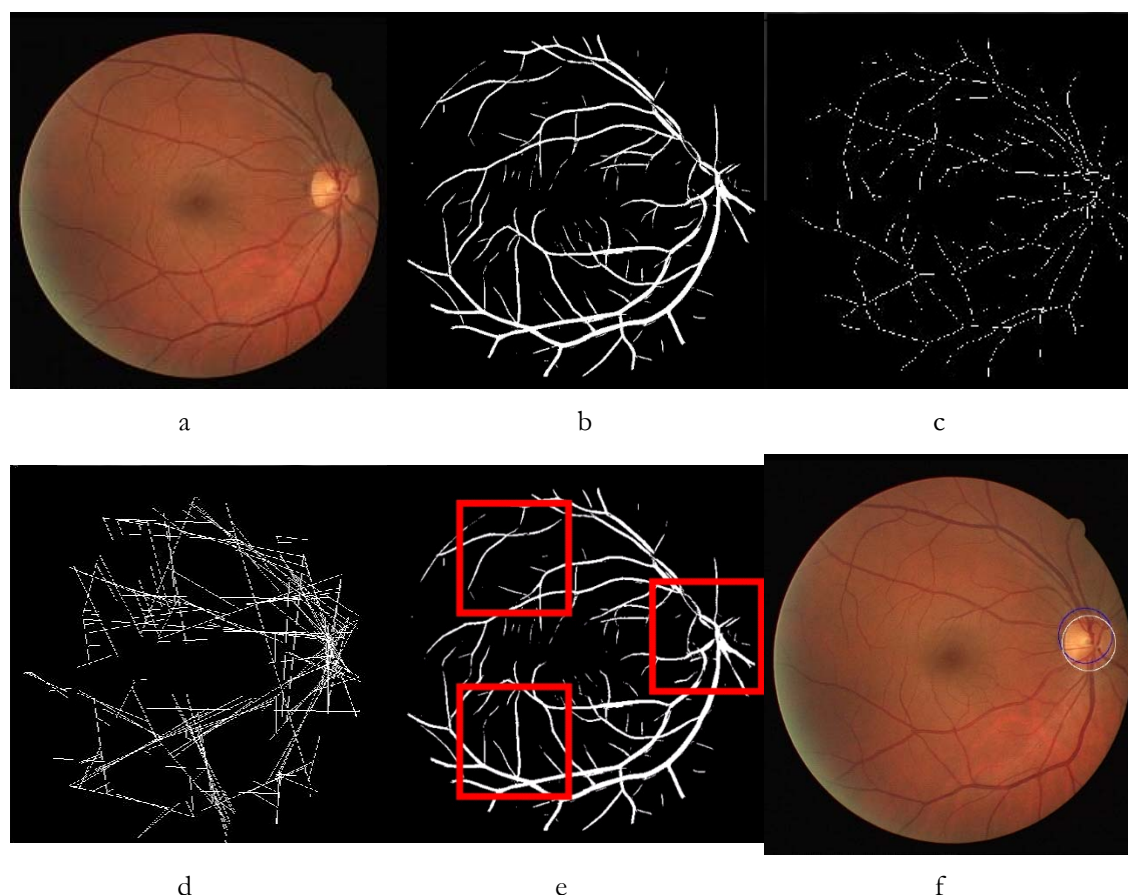

Figure 4 – Steps to OD detection: a) original image, b) vessel image, c) Skeletonization, d) Hough transform result, e) OD candidates, f) white circle in selected OD candidate.

C. Image Classification

According to the image evaluation definition, after the exudate-segmentation process, an image was classified as nonpathological if no candidate region was classified as exudate. If any candidate region was classified as exudate, then that image was labeled as pathological. However, even with the removal of several false candidates this strict analysis is susceptible to the presence of noise (small isolated regions). In this way, we used a second classification process to classify each image in pathological or nonpathological.

In this step, the algorithm extracts two attributes from each image: the number of regions segmented after the optic disc elimination and the number of candidates removed by the classification. Then, these attributes are used in a second classification process to classify each image into pathological or nonpathological.

RESULTS AND DISCUSSION

We tested our approach on the publicly available DIARETDB1 color fundus image database[14]. The DIARETDB1 consists of 89 images, all the same size (1500x1152). We chose this database to test algorithms for exudate detection because it provides the ground-truth spatial coordinates of findings related to four pathologies: hemorrhage, hard exudates, soft exudates and red spots[2]. Furthermore, it is a balanced database; i.e., the quantities of abnormal and normal images are similar.

The pathology marking was performed by four ophthalmologists. For several images, there was no consensus among all of them. Here, we considered only regions marked by at least three of the four ophthalmologists to be exudates, as suggested by the authors of DIARETDB1.

The performance evaluation of the exudate-detection algorithms considers three approaches: by image, by regions and pixel by pixel. In this study, we adopted the first two because the ground-truth images available in the database do not present a pixel-by-pixel correlation.

Assessment by image consists in verifying whether an image was classified as healthy (without exudates) or not (with exudates). The evaluation over regions validates a detected exudate candidate when it matches 50% of a region of the retinal image marked by the experts as exudate. This evaluation method was used by Ram and Sivaswamy[10], and it is consistent with the exudate characteristics, i.e., they are small, irregular and appear in group.

The performance evaluation of the classifiers is obtained in terms of the confusion matrix, which indicates the number of correct and incorrect classifications for each class, i.e., pathological and non-pathological. A confusion matrix contains four values: true positive (TP), the number of images or regions of exudates correctly detected; false positive (FP), the number of images or regions of non-exudates misdetected as exudate; false negative (FN), the number of images or regions of exudates not detected; and true negative (TN), the number of images or regions of non-exudates correctly identified. From these quantities, the sensitivity, specificity, accuracy and Fmeasure are computed. In this study, we also used the area under the ROC curve (AUC) and the Kappa coefficient. The accuracy degrees of the Kappa coefficient were established by Landis and Koch[15] in: Bad (K < 0.2), Reasonable (0.21 < K $< 0.4), Good (0.41 < K < 0.6), Very Good (0.61 < K < 0.8) and Excellent (K > 0.81).

We implemented and evaluated original algorithm developed by Ram and Sivaswamy[10] to demonstrate that the proposed changes produced improvements in the segmentation of exudate results. Table 1 shows the results of Ram and Sivaswamy[10] method and a modified version using fuzzy k-means in clustering stage and OD detection to remove false candidates.

The results in Table 1 show that the fuzzy k-means combined with the OD removal strategy implied an increase in the Kappa coefficient in both evaluation approaches, i.e., by image and by region. Comparative tests between k-means and its fuzzy version showed that the fuzzy k-means algorithm more accurately differentiated the lesions from other bright regions in the neighborhood. Therefore, the exudate candidates that resulted from the fuzzy k-means clustering were similar to those labeled by experts. Another improvement of this algorithm was the OD detection since this method avoided marking false candidates in the OD as exudate. The improvements in the modified algorithm increased the specificity due to the decreased of FP regions removed. However, more exudates regions also were remove, decreasing the sensitivity. Thus, the difference between the accuracy of the modified and the original algorithms was due to the FP reduction was much greater than the FN increasing.

It is noticed that the results of the image evaluation obtained inferior rates compared to the evaluation by regions. To cite two examples, the rates of SP and A were only 24.10% and 56.18%. This fact is due to the nature of the evaluation methodology that classifies a pathological image if there is at least one exudate in the final image. In this way, any noise in the image increases the false positives values. It is important to emphasize that in a real application the ophthalmologist will evaluate if

Table 1 - Evaluation by images and by regions of the original and modified algorithms.

	S	SP	A	FM	AUC	K
Original						
Imagens	100	20.85	52.81	66.10	61.20	0.18
Regions	84.94	98.45	73.90	82.70	88.30	0.81
Modified						
Imagens	97.22	24.10	56.18	66.10	66.60	0.19
Regions	80.31	99.44	99.25	84.32	90.80	0.83

the regions resulting from the segmentation (candidates for exudates) really are lesions. Thus, the evaluation by regions is more relevant to our problem. In order to reduce the number of false positives, we chose to perform a classification of all the existing regions after the OD identification step.

After OD identification, we have 6,835 candidate regions: 484 were exudates and 6,351 were non-exudates. We tested seven classifiers to eliminate the false-candidate regions. To statistically evaluate the classifier results, we used a hypothesis test (Z-test) with a significance of 5% to ascertain whether the tested classifiers were significantly different. Based on this test, we concluded that the C4.5, KNN, MLP and Random Forest achieved nearly the same performance and outperformed the others, i.e., RBF, Random Tree and SVM. Table 2 shows the best classifier evaluation results. The algorithms were tested using WEKA*[16] with 10-fold cross-validation as the evaluation method, and the chosen parameters were the defaults for each algorithm.

After the candidate classification, we finalize the exudate-segmentation process and evaluate the performance segmentations by region. Table 3 presents the four best results.

We used a hypothesis test with a significance of 5%, and we verified that the four classifiers achieved a significant similar performance. However, the Random Forest result was slightly superior to those of the other classifiers. Thus, we selected it to remove false-candidate regions.

We extracted two attributes from the segmented images: the number of regions before the first classification and the number of regions removed by the classification. In total, all retinal images were used to test the classifier. Then, we tested and compared the results of the classifiers C4.5, KNN, MLP, RBF, Random Forest, Random Tree

and SVM. Table 4 displays the best measures. The algorithms were tested using WEKA[16] with 10-fold cross-validation as the evaluation method, and the chosen parameters were the defaults for each algorithm.

According to a hypothesis test with a significance of 5%, the performance of the MLP was significantly better than that of the other classifiers. Hence, we selected the MLP to classify images as pathological or non-pathological.

When we observe the results of Ram and Sivaswamy[10] original algorithm and the results of our approach, we conclude that the changes suggested led to a performance gain in the main evaluation metrics. We can observe the increase in the Kappa coefficient when comparing it to the original algorithm introduced by Ram and Sivaswamy[10]. In the evaluation by regions (tables 1 and 3) our algorithm obtained a slightly better result, 0.86 against 0.81. On the other hand, in image evaluation (tables 1 and 4) there was a great performance gain. The Kappa coefficient of the original algorithm was "bad" (<0.21), whereas the proposed algorithm achieved a "very good" performance ($0.6 < K < 0.8$).

Additionally, the performance of the proposed algorithm outperformed the other methods reported in the literature, such as those described by, Walter et al.[17], Welfer et al.[7] and Akram et al.[8]. Figure 5 presents the image results of the proposed method for an image with exudate regions.

CONCLUSIONS

This paper introduces and extends a methodology for exudate detection in retinal images that combines clustering and false candidate elimination. After detecting the exudates, we tested different classifiers to classify an image according to pathological or non-pathological patterns,

Table 2 – Evaluation results of candidate classification.

	S	SP	A	FM	AUC	K
C4.5	77.90	98.90	97.40	81.25	92.40	0.80
KNN	78.10	99.20	97.70	82.71	95.00	0.80
MLP	**79.34**	98.72	97.35	81.00	95.10	0.80
Random Forest	78.10	**99.45**	**97.90**	**84.00**	**98.00**	**0.83**

Table 3 – Evaluation by region of the exudate detection after the candidate classification step.

	S	SP	A	FM	AUC	K
C4.5	79.20	99.88	99.87	85.68	91.10	0.84
KNN	79.25	99.84	99.83	85.32	90.80	0.84
MLP	79.19	99.87	99.86	85.24	90.75	0.83
Random Forest	**80.20**	**99.89**	**99.88**	**85.76**	**92.00**	**0.86**

Table 4 - Evaluation by image of the exudate detection after the image classification step.

	S	SP	A	FM	AUC	K
C4.5	73.10	83.30	77.30	79.20	73.00	0.55
KNN	80.80	83.30	81.80	84.00	77.00	0.63
MLP	**88.50**	**88.90**	**88.70**	**90.20**	**88.00**	**0.77**
Random Forest	69.20	55.60	63.70	69.30	56.00	0.25

---

* Weka is a free software for data mining with a collection of machine learning algorithms. It was developed by a group of researchers from the University of Waikato, New Zealand. Available in http://www.cs.waikato.ac.nz/ml/weka/
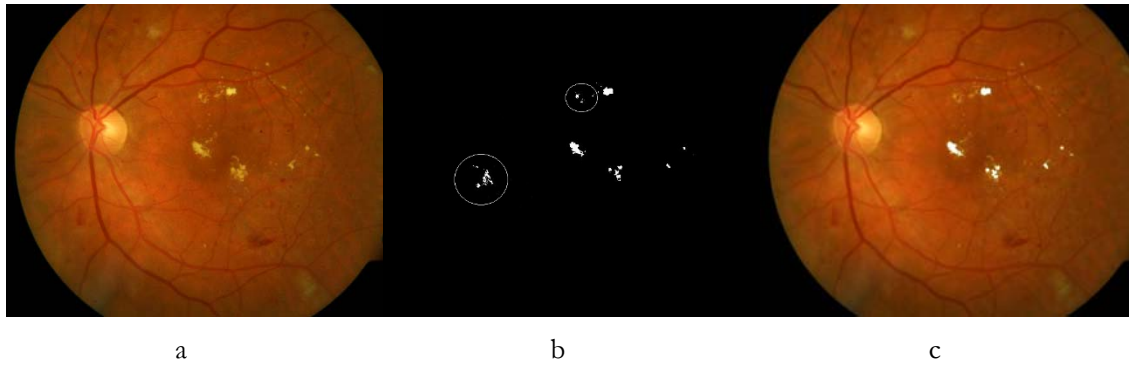
| a | b | c |

Figure 5 – Results of the new algorithm: a) original image, b) candidate regions before classification step (the region marked with a white circle contains false candidates), c) overlay of the result on the original image

and the MLP achieved the best performance.

The success of the proposed algorithm is due mostly to the OD detection approach and the classification step. The proposed method of OD detection is based on the fact that there is a convergence point of vessels. After removing the OD, seven classifiers were tested to eliminate false candidates, and the Random Forest outperformed (Kappa of 0.83) the others. This classifier was actually more effective in eliminating false candidates in this set of fundus images than the others. After detecting the exudates, the images were classified according to pathological and non-pathological patterns.

Future studies will use the principal component analysis (PCA) to eliminate feature correlation and therefore improve the classification process, decrease the MLP complexity and increase its efficiency. Moreover, we will test ensembles of classifiers and other image features with the aim of increasing the efficiency of classification.

REFERENCES

1. Bernardes R, Serranho P, Lobo C. Digital ocular fundus imaging: a review. Ophthalmologica. 2011; 226(4):161-81.
2. Giancardo L, Meriaudeau F, Karnowski TP, Li Y, Garg S, Tobin KW, Chaum E. Exudate-based diabetic macular edema detection in fundus images using publicly available datasets. Med Image Anal. 2012;16(1):216-26.
3. Amos AF, McCarty DJ, Zimmet P. The rising global burden of diabetes and its complications: estimates and projections to the year 2010. Diabetic medicine: J British Diabetic Association.1997;14 (Suppl 5): S1-S5.
4. Sopharak A, Dailey NM, Uyyanonvara B, Barman S, Williamson T, New TN, Moe AY. Machine learning approach to automatic exudate detection in retinal images from diabetic patients. J Mod Opt. 2010; 57(2):124-35.
5. García M, Sánchez CI, Lopez I, Abásolo H, Hornero R. Neural network based detection of hard exudates in retinal images. Comput Methods Programs Biomed. 2009;93(1):9-19.
6. Harangi B, Antal B, Hajdu A. Automatic exudate detection with improved naive bayes classifier. Proceedings of the IEEE International Symposium on Computer-Based Medical System; 2012 Jun 20-22; Rome, Italy.
7. Welfer D, Scharcanski J, Marinho DR. A coarse-to-fine strategy for automatically detecting exudates in color eye fundus images. Comput Med Imaging Graph. 2010;34(3):228-35.
8. Akram MU, A Tariq, Khan SA, Javed MY. Automated detection of exudates and macula for grading of diabetic macular edema. Comput Methods Programs Biomed. 2014;114(2):141-52.
9. Rocha A, Carvalho T, Jelinek H, Goldenstein S, Wainer J.

Points of interest and visual dictionaries for automatic retinal lesion detection. IEEE Trans Biomed Eng. 2012;59(8):2244-53.
10. Ram K, Sivaswamy J. Multi-space clustering for segmentation of exudates in retinal color photographs. Proceedings of the 32nd Annual International Conference of the IEEE Engineering in Medicine and Biology; 2009 Sept 3-6: Minneapolis, Minnesota. p.1437-40.
11. Zana F, Klein JC. Segmentation of vessel-like patterns using mathematical morphology and curvature evaluation. IEEE Trans Image Process. 2001;10(7):1010-9.
12. Rokach L, Maimon O. Data Mining with decision trees: theroy and applications. River Edge, NJ, USA: World Scientific Publishing Co., Inc.; 2008.
13. Haykin S. Neural networks: a comprehensive foundation. 2nd ed. Prentice Hall; 2001.
14. Kauppi T, Kalesnykiene V, Kamarainen JK, Lensu L, Sorri I, Kalviainen H, Pietila J. Diaretdb1 diabetic retinopathy database and evaluation protocol. In: Proceedings of the Conference on Medical Image Understanding and Analysis. British Machine Vision Association; 2007 Sept 10-13; University of Warwick, **UK**.
15. Landis J, Koch G. The measurement of observer agreement for categorical data. Biometrics. 1977;33(1):159-74.
16. Witten IH, Frank E, Hall MA. Data Mining: practical machine learning tools and techniques. 3rd ed. Canadá: Morgan Kaufmann; 2011.
17. Walter T, Klevin J, Massin P, Erginay A. A contribution of image processing to the diagnosis of diabetic retinopathy-detection of exudates in color fundus images of the human retina. IEEE Trans Med Imag. 2002;21(10):1236-43.